Accepted for publication, cite as: Bradley BA. Site-specific and spatially-distributed ground-motion intensity estimation in the 2010–2011 Canterbury earthquakes. *Soil Dynamics and Earthquake Engineering* 2014; **61–62** (0): 83-91.

SITE-SPECIFIC AND SPATIALLY-DISTRIBUTED GROUND-MOTION INTENSITY ESTIMATION IN THE 2010-2011 CANTERBURY EARTHQUAKES

Brendon A Bradley[1]

[1]Department of Civil and Natural Resources Engineering, University of Canterbury, Private Bag 4800, Christchurch, New Zealand

[*]Ph +64 3 364 2987 x 7395, brendon.bradley@canterbury.ac.nz

ABSTRACT

This paper presents site-specific and spatially-distributed ground-motion intensity estimates which have been utilized in the aftermath of the 2010-2011 Canterbury, New Zealand earthquakes. The methodology underpinning the ground motion intensity estimation makes use of both prediction models for ground motion intensity and its within-event spatial correlation. A key benefit of the methodology is that the estimated ground motion intensity at a given location is not a single value but a distribution of values. The distribution is comprised of both a mean and standard deviation, with the standard deviation being a function of the distance to nearby observations at strong motion stations.

The methodology is illustrated for two applications. Firstly, maps of conditional peak ground acceleration (PGA) have been developed for the major events in the Canterbury earthquake sequence, which among other things, have been utilized for assessing liquefaction triggering susceptibility of land in residential areas. Secondly, the conditional distribution of response spectral ordinates is obtained at the location of the Canterbury Television building (CTV), which catastrophically collapsed in the 22 February 2011 earthquake. The conditional response spectra provide insight for the selection of ground motion records for use in forensic seismic response analyses of important structures at locations where direct recordings are absent.

INTRODUCTION

Earthquake-induced strong ground motions recorded on the surface occur as a result of complex rupture on a fault; wave propagation through the Earth's heterogeneous crust; and further modification resulting from the nonlinear response of surficial soils, whose characteristics vary spatially over distances of several meters.

Accepted for publication, cite as: Bradley BA. Site-specific and spatially-distributed ground-motion intensity estimation in the 2010–2011 Canterbury earthquakes. *Soil Dynamics and Earthquake Engineering* 2014; **61–62** (0): 83-91.

Thus, it is not surprising that earthquake-induced ground motions exhibit significant spatial variability over distances of interest. The spatial variability of earthquake-induced ground motion intensity measures (IMs) has been investigated by numerous researchers. Within-event (also referred to as intra-event) spatial correlations have been examined by Boore et al. [1], using peak ground acceleration (PGA) values from the 1994 Northridge earthquake; Wang and Tanaka [2], using peak ground velocity (PGV) values for six Japanese earthquakes; Goda and Hong [3], using PGA and pseudo-spectral acceleration (SA) values in ground motions from California and Taiwan; and Jayaram and Baker [4] and Loth and Baker [5], using SA values for seven and eight different shallow crustal earthquake events, respectively.

Within-event spatial correlation models for ground motion IMs have been principally used for simulating spatially correlated random fields of ground motion IMs as part of risk assessments of spatially distributed infrastructure, e.g. Park et al. [6], Jayaram [7], among others. While these applications are generally for the prediction of future earthquake events, an understanding of the spatial characteristics of ground motion intensity can also be utilized to infer the spatial distribution of ground motion intensity from an event which has already occurred, both in the immediate response phase for the triaging of building and other infrastructure inspections, as well as for providing seismological information required for performance reconciliation of important case histories.

Bommer and Stafford [8] provide a general discussion on approaches by which one may attempt to develop an estimate of the ground motion at a specific site resulting from an earthquake event using several potential datasets (including strong motion station observations which will be the sole focus herein). Stafford [9] provides one such application for the estimation of spatially averaged elastic spectral displacements over a discretely gridded region of Christchurch city resulting from the 22 February 2011 $M_w 6.2$ Christchurch earthquake, while Bhattachrya and Goda [10] recently used a similar approach to estimate PGA for pile foundation assessment.

This paper presents site-specific and spatially distributed estimates of instrumental measures of ground motion intensity from the Canterbury earthquakes which have been utilized for decision making purposes in the aftermath of these events. First, the theory underpinning the conditional ground motion IM estimation is presented. Second, the specific applications of: (i) estimation of the conditional distribution of PGA over the entire urban Christchurch region for liquefaction

Accepted for publication, cite as: Bradley BA. Site-specific and spatially-distributed ground-motion intensity estimation in the 2010–2011 Canterbury earthquakes. *Soil Dynamics and Earthquake Engineering* 2014; **61–62** (0): 83-91.
assessment; and (ii) site-specific estimation of response spectra for the forensic examination of the Canterbury Television (CTV) building collapse are presented.

CONDITIONAL GROUND MOTION DISTRIBUTION THEORY

Because of the complexity of a ground motion time series, the engineering representation of ground motion severity typically comprises one or more ground motion intensity measures, *IM*. Below the general *IM* variable will be used, while subsequent applications will make use of a specific IM (e.g. *PGA*, or pseudo-acceleration response spectral ordinates, *SA*).

The representation of an *IM* from earthquake event *e*, at a single location *s*, for the purposes of ground motion prediction is generally given by:

$$lnIM_{es} = \overline{lnIM_{es}}(Site, Rup) + \delta B_e + \delta W_{es} \quad (1)$$

where $lnIM_{es}$ is the (natural) logarithm of the observed IM ; $\overline{lnIM_{es}}(Site, Rup)$ is the mean of $lnIM$ (equal to the median of *IM* for a lognormal distribution) as given by an empirical ground motion prediction equation (GMPE), which is a function of the site and earthquake rupture ("Rup") considered (i.e. rupture magnitude and geometry, source-to-site distance etc.); δB_e is the between-event residual with zero mean and variance σ_B^2; and δW_{es} is the within-event residual for location *s* with zero mean and variance σ_W^2. Based on Equation (1), empirical ground motion prediction equations provide the (unconditional) distribution of ground motion intensity as:

$$lnIM_{es} \sim N(\overline{lnIM_{es}}, \sigma_B^2 + \sigma_W^2) \quad (2)$$

where $X \sim N(\mu_X, \sigma_X^2)$ is short-hand notation for X having a normal distribution with mean μ_X and variance σ_X^2.

By definition, for a given ground motion intensity measure, IM, all observations from a single earthquake event have the same between-event residual, δB_e. In this regard, δB_e represents the correlation between all observations from a single event which subsequently affects the ground motion at all considered locations in a systematic manner. On the other hand, the within-event residual, δW_{es}, varies from site to site, and hence represents all other factors which lead to a difference between the observed ground motion IM, the predicted mean, and the between-event residual. While the within-event residual varies in value from site to site, it is correlated spatially as a result of similarities of path and site effects between various locations

[1-4].

Based on the aforementioned properties of δB_e and δW_{es}, use can be made of recorded *IM* values at strong motion stations to compute the conditional distribution of *IM* at an arbitrary site of interest on the basis that the spatial field of ground motion IM, for a given earthquake event, is well represented by a multivariate lognormal distribution (i.e. $lnIM$ has a multivariate normal distribution) [9]. Firstly, a GMPE is used to compute the unconditional distribution of ground motion intensity at the strong motion stations where ground motions were recorded. The between-event residual can then be computed from [11]:

$$\delta B_e = \frac{\mathbf{1}_{n,1}^T \boldsymbol{C_C^{-1}} \boldsymbol{\xi}}{\frac{1}{\sigma_B^2} + \mathbf{1}_{n,1}^T \boldsymbol{C_C^{-1}} \mathbf{1}_{n,1}} \tag{3}$$

where $\mathbf{1}_{n,1}$ is a column vector of ones, where n is the number of ground motion records considered for the event; $\boldsymbol{\xi}$ is a column vector of the total residuals (i.e. $\boldsymbol{\xi} = \boldsymbol{lnIM} - \overline{\boldsymbol{lnIM}}$); and $\boldsymbol{C_C}$ is the covariance matrix of the within-event residuals. The i^{th} row and j^{th} column of $\boldsymbol{C_c}$, which provides the correlation between the within-event residuals of the i^{th} and j^{th} strong motion station observations is given by:

$$\boldsymbol{C_c}(i,j) = \rho_{i,j} \sigma_{W_{ei}} \sigma_{W_{ej}} \tag{4}$$

where $\rho_{i,j}$ is the spatial correlation of the within-event residuals, which can be obtained from empirical equations given elsewhere [1-4]. Once the between-event residual is computed via Equation (3), the within-event residuals at all of the strong motion stations can be computed via Equation (1).

The conditional distribution of ground motion at a specific site, *s*, at which no strong motion stations exist will differ from the unconditional distribution (i.e. Equation (2)) because of the non-zero value of the between-event residual, and the spatial correlation of the within-event residuals. The joint distribution of within-event residuals at this site of interest and the considered strong motion stations can be represented by:

$$\begin{bmatrix} \delta W_{es} \\ -- \\ \boldsymbol{\delta W_{eSMS}} \end{bmatrix} = N\left(\begin{bmatrix} 0 \\ -- \\ \mathbf{0} \end{bmatrix}, \begin{bmatrix} \sigma_{W_{es}}^2 & | & \boldsymbol{\Sigma}_{12} \\ -- & + & -- \\ \boldsymbol{\Sigma}_{21} & | & \boldsymbol{\Sigma}_{22} \end{bmatrix} \right) \tag{5}$$

where $\boldsymbol{X} \sim N(\boldsymbol{\mu_X}, \boldsymbol{\Sigma})$ is short-hand notation for $\boldsymbol{X}$ having a multivariate normal

distribution with mean $\boldsymbol{\mu_X}$ and covariance matrix $\boldsymbol{\Sigma}$ (i.e. as before, but in vector form); $\boldsymbol{\delta W_{eSMS}}$ is a column vector of the within-event residuals at all of the strong motion stations (SMS); and $\sigma^2_{W_{es}}$ is the variance in the within-event residual at the site of interest. In Equation (5), matrices are expressed in a partitioned fashion to elucidate the subsequent computation of the conditional distribution of δW_{es}. It should be noted, in particular, that $\boldsymbol{\Sigma_{22}} = \boldsymbol{C_C}$, while the remaining elements of the covariance matrix in Equation (5) can be computed similar to Equation (4).

Based on the joint distribution of within-event residuals given by Equation (5), the conditional distribution of δW_{es} can be computed from [11, 12]:

$$[\delta W_{es}|\boldsymbol{\delta W_{eSMS}}] = N\left(\boldsymbol{\Sigma}_{12}\cdot\boldsymbol{\Sigma}_{22}^{-1}\cdot\boldsymbol{\delta W_{eSMS}},\ \sigma^2_{W_{es}} - \boldsymbol{\Sigma}_{12}\cdot\boldsymbol{\Sigma}_{22}^{-1}\cdot\boldsymbol{\Sigma}_{21}\right) \quad (6)$$

$$= N\left(\mu_{\delta \mathrm{W_{es}}|\boldsymbol{\delta W_{eSMS}}},\ \sigma^2_{\delta \mathrm{W_{es}}|\boldsymbol{\delta W_{eSMS}}}\right)$$

Finally, using the conditional distribution of the within-event residual at the site of interest given by Equation (6), and substituting into Equation (2), the conditional distribution at the site of interest, IM_{es}, can be computed from:

$$\left[lnIM_{es}\middle|ln\boldsymbol{IM_{eSMS}}\right] = \quad (7)$$

$$N\left(\overline{lnIM_{es}} + \delta B_e + \mu_{\delta \mathrm{W_{es}}|\boldsymbol{\delta W_{eSMS}}},\ \sigma^2_{\delta \mathrm{W_{es}}|\boldsymbol{\delta W_{eSMS}}}\right)$$

That is, the conditional distribution of the IM at a specific site is a lognormal random variable which is completely defined via the conditional mean and conditional standard deviation.

It should be noted that in cases where the site of interest is located far from any strong motion stations, the conditional distribution will be similar to the unconditional distribution; and for sites of interest located very close to a strong motion station, the conditional distribution will approach the value observed at the strong motion station.

Equations (5)-(7), as written, provide the conditional IM distribution at a single location and can easily be applied sequentially over an array of sites of interest for the cases herein in which only the marginal distribution of IM at each site is of concern. For cases in which the joint distribution of the IM at these array of sites is of interest the above approach can be easily expanded [9]. The subsequent sections present applications of the above theory for conditional ground motion IM estimation in the Canterbury earthquakes and discuss their role in decision making.

Accepted for publication, cite as: Bradley BA. Site-specific and spatially-distributed ground-motion intensity estimation in the 2010–2011 Canterbury earthquakes. *Soil Dynamics and Earthquake Engineering* 2014; **61–62** (0): 83-91.

SPATIAL PGA MAPS IN THE CANTERBURY EARTHQUAKES

One of the prevalent aspects of the 2010-2011 Canterbury earthquakes was the severity and spatial extent of liquefaction in native soils which occurred in multiple events [13-16]. Immediately following earthquake events, Tonkin and Taylor [17] undertook residential housing and land damage surveys of the region in order to enable quantification of liquefaction-related damage for subsequent insurance claims through the New Zealand Earthquake Commission (EQC). In order to remediate land damage, geotechnical assessments were needed to assess the liquefaction resistance of surficial soils in residential areas. Usually this would be achieved by conventional simplified liquefaction triggering procedures [e.g. 18]. However, the occurrence of multiple events in a region with both dense seismic instrumentation and well documented post-earthquake damage allows for the possibility of assessing liquefaction resistance on the basis of observations in conjunction with information from simplified empirical equations [e.g. 19, Figure 28]. A key ingredient for such an assessment is the estimated PGA experienced at each site, which is utilized to compute the cyclic stress ratio (CSR) of the imposed ground motion [18]. This section discusses the earthquake sources of the events considered, and the GMPEs and spatial correlation equations which were adopted to compute the spatial maps of PGA.

Earthquake sources considered

Figure 1 illustrates the finite faults of major earthquakes in the Canterbury earthquake sequence for which spatially-distributed maps of conditional PGA values have been developed. The finite fault models for the 4 September 2010, 22 February 2011, 13 June 2011 (2:20pm) and 23 December 2011 (2:18pm) events are from Beavan et al. [20], while those for the 16 April 2011, 13 June 2011 (1:01pm), and 23 December 2011 (2:18pm) events were obtained in a first-order manner by using the centroid moment tensor (CMT) solutions from the GeoNet catalogue [21], and then fault dimensions based on magnitude scaling relationships [22].

Peak ground accelerations observed in the Canterbury earthquakes and comparison with empirical predictions

In order to accurately estimate the conditional PGAs in the Canterbury

earthquakes it is necessary to utilize an empirical GMPE which is both unbiased and has the correct precision with respect to strong motion station observations. Several studies have examined the performance of GMPEs with respect to the ground motions from various events in the Canterbury earthquake sequence [23-27].

Figure 2 illustrates the PGA observations for the 7 considered events as compared to the New Zealand (NZ)-specific site class D prediction of Bradley [28, 29] (herein "Bradley (2010)"), while Table 1 provides the numerical values of observed PGA's in the urban Christchurch region at strong motion stations during the Canterbury earthquakes [25, 30]. It should be noted that the maximum source-to-site distance considered for each event in Figure 2 was magnitude dependent, in order to ensure that emphasis is given to the prediction of ground motion amplitudes of engineering importance (as elaborated upon in [27]). On the basis of Figure 2 it can be seen that the Bradley (2010) model: (i) exhibits good scaling of PGA amplitudes with source-to-site distance, R_{rup}, even for very near-source distances; and (ii) provides a consistent prediction of ground motions from events of different magnitudes. The same trends for PGA are also apparent for SA at various vibration periods presented elsewhere [31, Appendix 1]. For these reasons the Bradley (2010) model was adopted to obtain the subsequently presented results. Nonetheless, while the observations are, on average, consistent with the empirical prediction, there is significant scatter in the observations as a result of complex source, path and site effects. Because the conditional PGA values computed subsequently account for the spatial correlation in within-event residuals, and hence the site-to-site variability, then they attempt to account for this localized variability in PGA values.

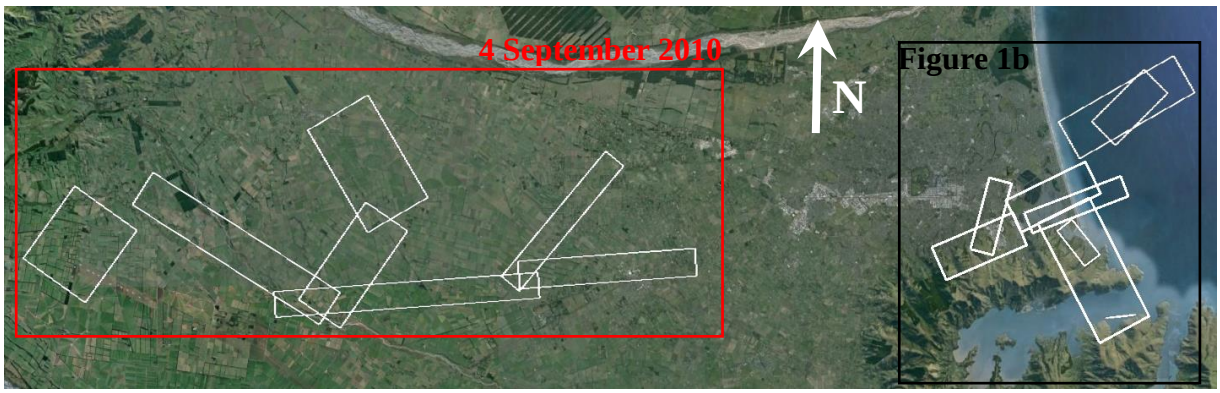

Accepted for publication, cite as: Bradley BA. Site-specific and spatially-distributed ground-motion intensity estimation in the 2010–2011 Canterbury earthquakes. *Soil Dynamics and Earthquake Engineering* 2014; **61–62** (0): 83-91.

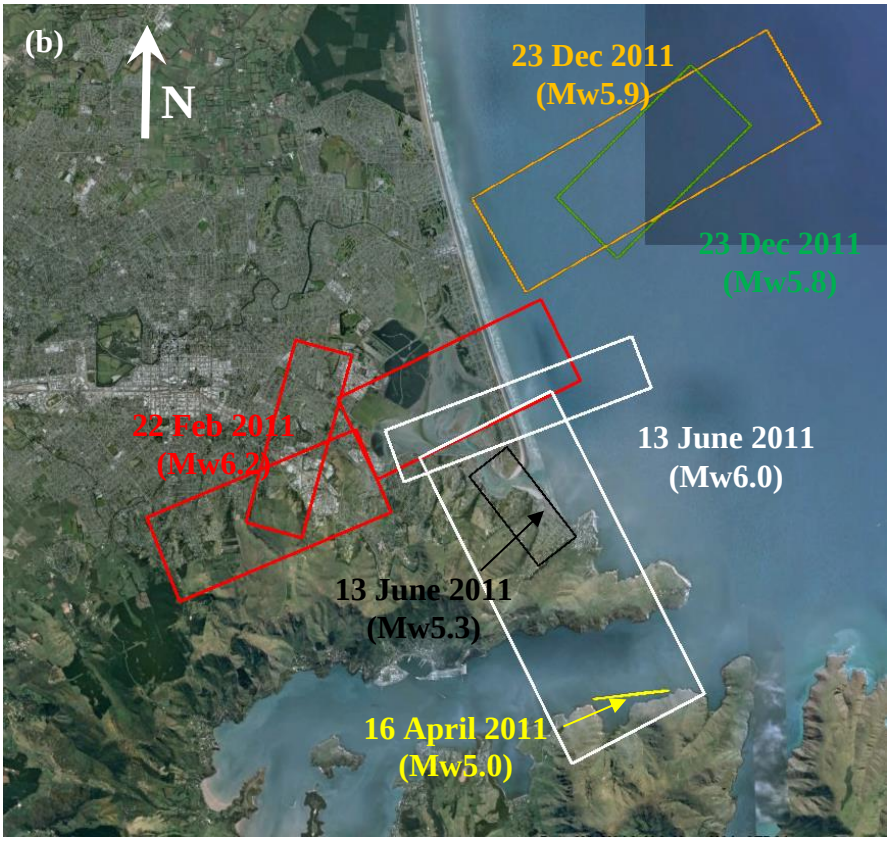

Figure 1: Finite faults from the seven major events in the Canterbury earthquake sequence for which spatial maps of PGA have been developed: (a) regional Canterbury view; and (b) local Christchurch view.

Spatial correlation of within-event residuals

Empirical analysis of ground motion data worldwide, illustrate that within-event residuals are spatially correlated. This is inferred physically as the result of similarity in path and site effects at geographically proximate locations. The correlation of ground motion SA amplitudes is vibration period-dependent since the natural frequency of waves is proportional to the length of the waves, and therefore the spatial distances over which waves are expected to be relatively coherent due to source, path and site effects.

The spatial correlation of within-event residuals for PGA and SA were examined using empirical data from the Canterbury earthquakes. Figure 3 compares, for example, the empirical correlation of PGA within-event residuals from the 22 February 2011 and 4 September 2010 earthquakes as a function of separation distance with respect to the empirical correlation equations provided by Goda and Hong [3], Jayaram and Baker [4] and Loth and Baker [5]. As the Loth and Baker equation is only valid for SA values, then the correlation between PGA values at two sites is based on the approximation, $PGA \approx SA(0.01s)$. The presented empirical results are

based on the computed semi-variogram [e.g. 4] using a bin width of 3km for the separation distance. Smaller bin widths were found to produce unstable results due to a lack of data within each bin. Comparison of the empirical data and the prediction equations illustrates that all three models do a relatively good job of capturing the empirical correlation at short separation distances ($\Delta < 5km$), which is the most important for applications [4], although the Loth and Baker prediction is notably different as the separation distance increases. Although not considered here, other spatial correlation models which have focused more specifically on smaller separation distances (e.g. [32, 33]) may yield useful future insights.

It should be noted that at the time the applications in this paper were first developed (August 2011), the Loth and Baker [5] prediction shown in Figure 3 was not published and therefore only the Goda and Hong [3] and Jayaram and Baker [4] were potential candidate models. Although both of these models cannot be distinguished on the basis of the comparison with empirical data from the Canterbury earthquakes, the Goda and Hong model was adopted because of its lower predicted correlations for very small separation distances ($\Delta < 1km$), e.g. at $\Delta = 0.5km$ the Goda and Hong and Jayaram and Baker models yield $\rho \sim 0.5$ and $\rho \sim 0.85$, respectively. For the Christchurch central business district, where multiple strong motion stations are in close proximity, use of the Jayaram and Baker model yielded unrealistically small (near zero) values of the conditional standard of PGA. Thus, this highlights the need to further constrain the correlation of ground motion IM values for very small separation distances, where empirical data is sparse.

Accepted for publication, cite as: Bradley BA. Site-specific and spatially-distributed ground-motion intensity estimation in the 2010–2011 Canterbury earthquakes. *Soil Dynamics and Earthquake Engineering* 2014; **61–62** (0): 83-91.

Table 1: Observed values of PGA at strong motion stations in the urban Christchurch area which were utilized for developing the conditional PGA maps

Station	Site class[1]	Observed geometric mean peak ground acceleration in each event, PGA (g)						
		04/09/10	22/02/11	16/04/11	13/06/11(a)	13/06/11(b)	23/12/11(a)	23/12/11(b)
CACS	D	0.197	0.21	0.034	0.081	0.136	0.073	0.083
CBGS	D	0.158	0.50	0.070	0.183	0.163	0.157	0.210
CCCC	D	0.224	0.43	-	-	-	0.134	0.179
CHHC	D	0.173	0.37	0.146	0.199	0.215	0.174	0.222
CMHS	D	0.237	0.37	0.137	0.159	0.178	0.152	0.174
HPSC	E	0.147	0.22	0.148	0.180	0.256	0.199	0.264
HVSC	C	0.606	1.41	0.676	0.455	0.914	0.306	0.439
KPOC	D	0.339	0.20	0.052	0.186	0.099	-	-
LINC	D	0.437	0.12	0.028	0.026	0.065	0.062	0.073
LPCC	D	0.290	0.92	0.294	0.146	0.639	-	0.437
NBLC	D	-	-	0.129	0.232	0.214	0.201	-
NNBS	E	0.206	0.67	0.156	0.239	0.198	-	-
PPHS	D	0.221	0.21	0.062	0.118	0.122	0.116	0.138
PRPC	E	0.214	0.63	0.223	0.299	0.341	0.290	-
REHS	D	0.252	0.52	0.101	0.188	0.264	0.204	0.254
RHSC	D	0.210	0.28	0.075	0.083	0.194	0.159	0.159
ROLC	D	0.340	0.18	0.013	0.036	0.045	0.102	0.062
SHLC	D	0.175	0.33	0.116	0.245	0.184	0.262	0.275
SMTC	D	0.176	0.16	0.034	0.132	0.085	0.066	0.148
TPLC	D	0.266	0.11	0.024	0.037	0.065	0.068	0.081

[1]As defined by the New Zealand Loadings Standard, NZS1170.5 [34], i.e. B=rock, C=shallow soil, D=deep or soft soil, E=very soft soil

Accepted for publication, cite as: Bradley BA. Site-specific and spatially-distributed ground-motion intensity estimation in the 2010–2011 Canterbury earthquakes. *Soil Dynamics and Earthquake Engineering* 2014; **61–62** (0): 83-91.

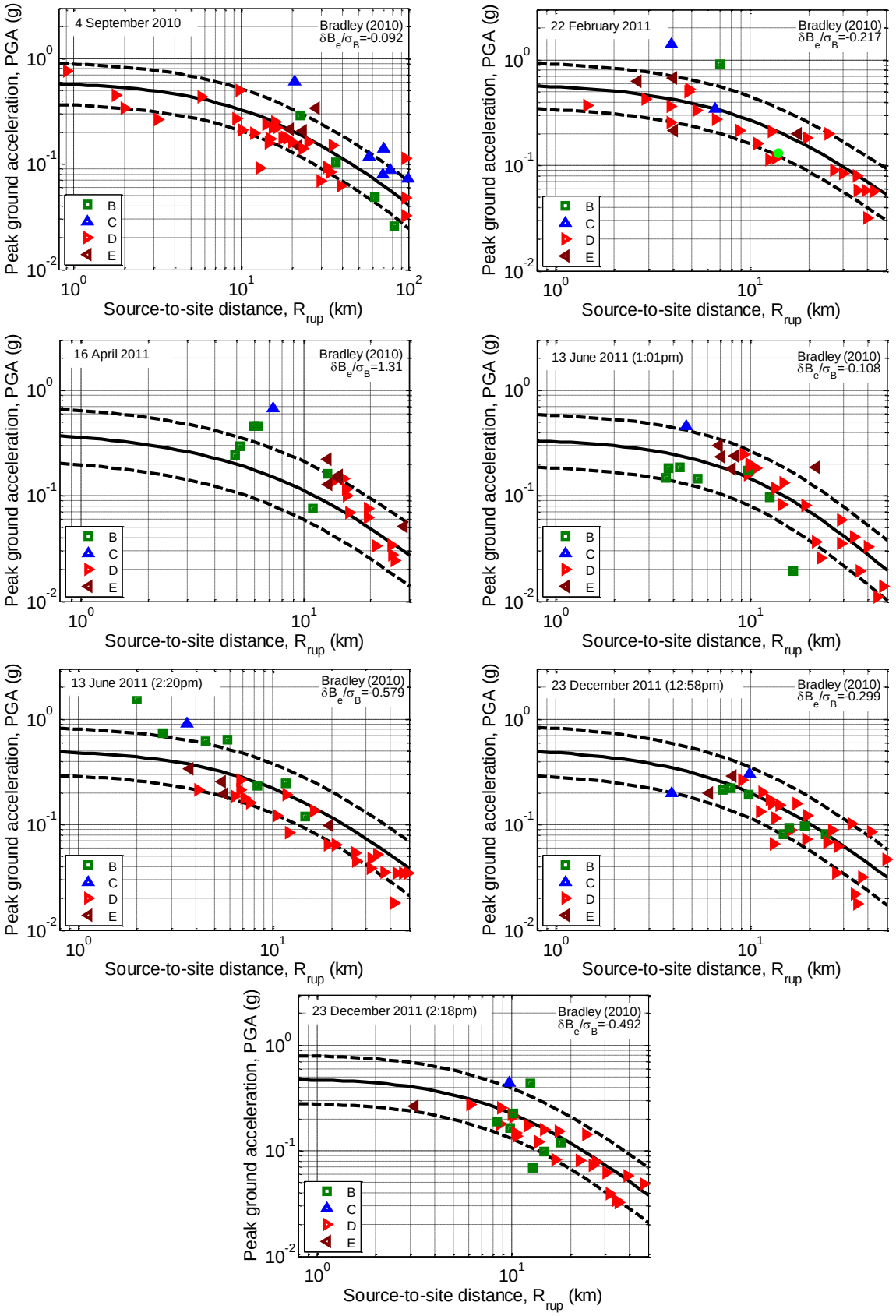

Figure 2: Comparison of the Bradley (2010) GMPE (prediction shown for site class D) with PGA observations from the 7 considered events (event names given in the upper left of each figure). Denoted values of the between-event residual, δB_e, are normalized by the between-event standard deviation, σ_B, so that $\delta B_e/\sigma_B = +1.0$ implies observations with an between-event residual which is one standard deviation above zero.

Accepted for publication, cite as: Bradley BA. Site-specific and spatially-distributed ground-motion intensity estimation in the 2010–2011 Canterbury earthquakes. *Soil Dynamics and Earthquake Engineering* 2014; **61–62** (0): 83-91.

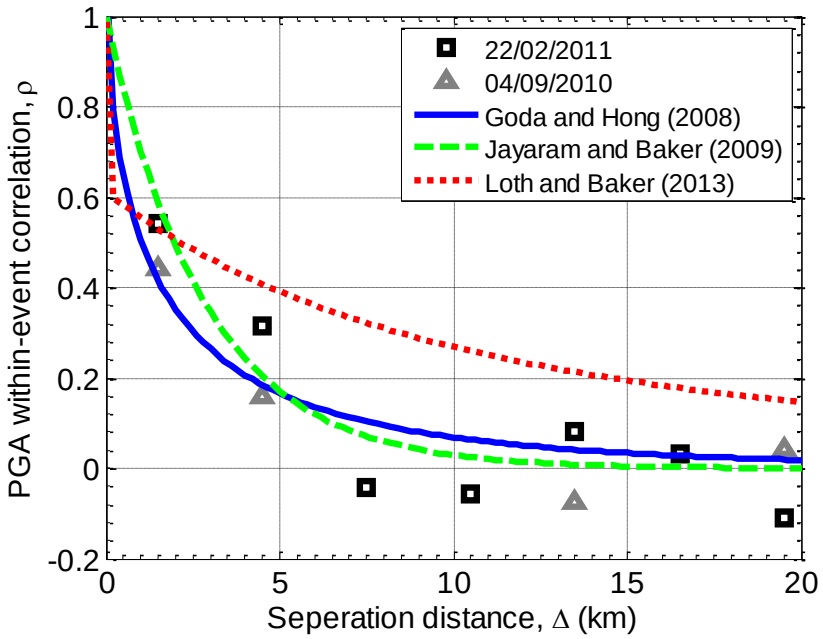

Figure 3: Correlation of within-event resduals for PGA as a function of seperation distance. Empirical values based on a discrete bin width of 3km.

Computed spatial PGA maps for the Canterbury earthquakes

Figure 4 and Figure 5 provide examples of the spatial PGA maps produced for the 4 September 2010 and 22 February 2011 earthquakes, respectively, which have been adopted by the Engineering Advisory Group to the Ministry of Business, Innovation and Employment (MBIE) [35] for liquefaction evaluation. These figures are directly obtained from the publically available Canterbury Geotechnical Database [17], in which the results for all 7 earthquake events are available. In Figure 4 and Figure 5, the median PGA values are portrayed by contours, while the standard deviation is given according to the color map in the figure legend. Several features are worthy of note in Figure 4 and Figure 5:

- The median PGA amplitudes display a typical attenuation as the distance from the earthquake source increases.
- In the proximity of strong ground motion stations, the contours can be observed to vary markedly as a result of differences between some observed PGA. This is consistently the case in Heathcote Valley for all events, for example, due to strong basin-edge effects [24]. However, as shown by the median PGA contours, such effects are expected to be spatially localised.
- The conditional standard deviations provide an indication of the level of uncertainty in the conditional median PGA prediction. Near strong motion stations the conditional standard deviations decrease toward zero, implying that the predicted

PGAs values are more accurate close to strong motion stations, and less accurate as the distance from strong motion stations increases, as would be expected.

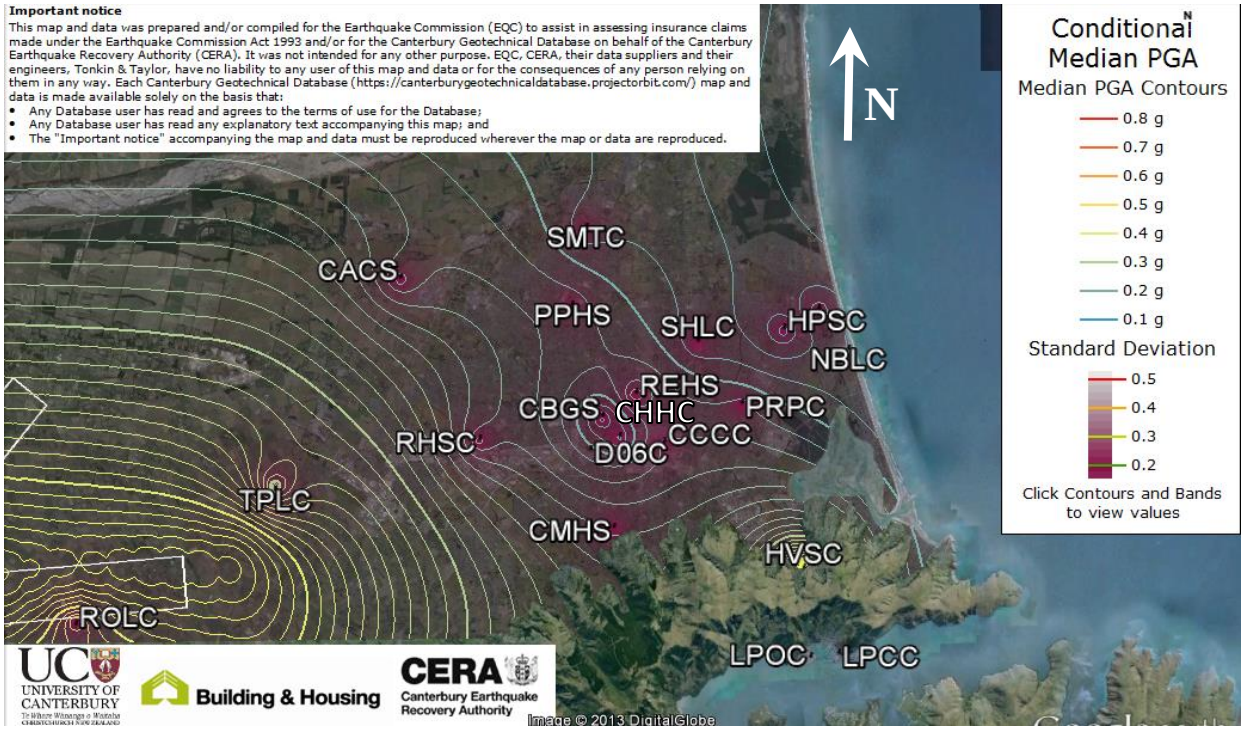

Figure 4: Conditional median and standard deviation values of PGA predicted in Canterbury from the 4 September 2010 earthquake.

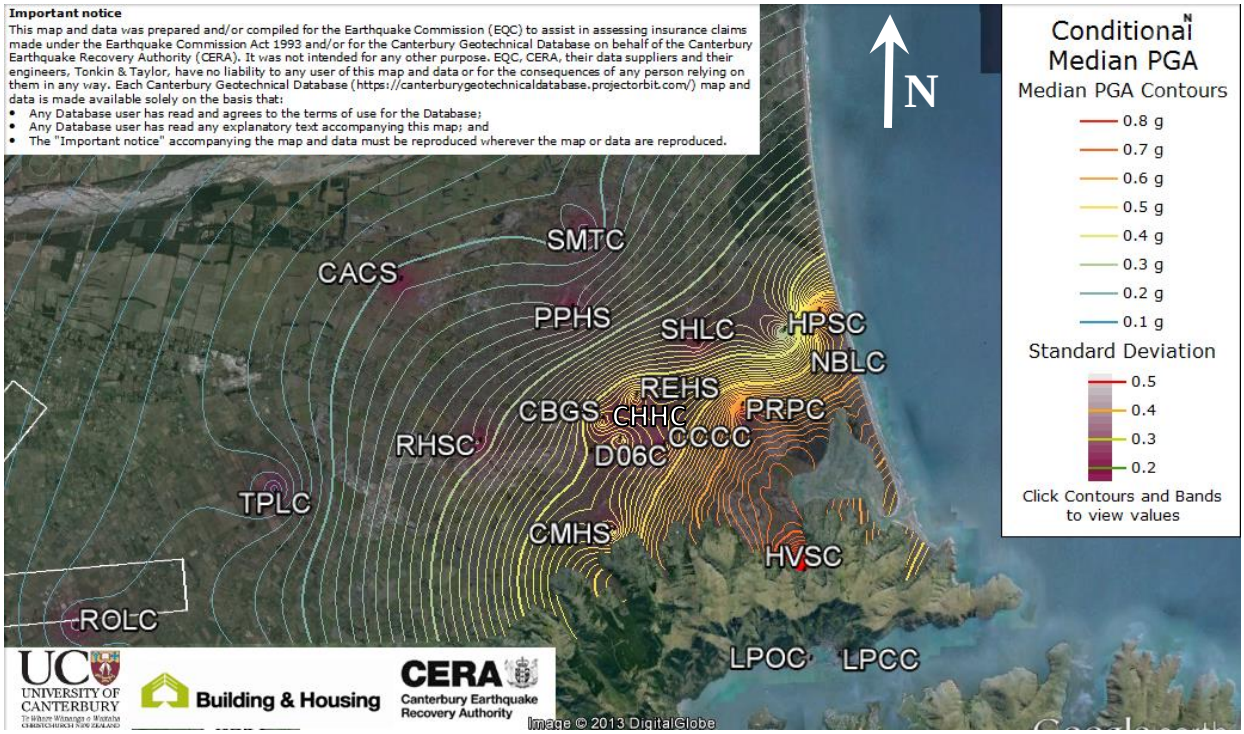

Figure 5: Conditional median and standard deviation values of PGA predicted in Canterbury from the 22 February 2011 earthquake.

Accepted for publication, cite as: Bradley BA. Site-specific and spatially-distributed ground-motion intensity estimation in the 2010–2011 Canterbury earthquakes. *Soil Dynamics and Earthquake Engineering* 2014; **61–62** (0): 83-91.

CONDITIONAL RESPONSE SPECTRA VALUES FOR SITE-SPECIFIC FORENSIC ASSESSMENTS

The aforementioned theory can also be used to examine the prediction of response spectral ordinates of different vibration periods, $SA(T)$, at a specific location. Such predictions can therefore provide a site-specific estimate of the response spectrum of the unknown ground motion which occurred during these past events. The same is true for other measures of ground motion intensity, although attention here is restricted to SA values. For each vibration period considered only the spatial correlation and observed values of $SA(T)$ are considered to determine the site-specific estimate of $SA(T)$. That is, spatial cross-correlation between different response spectral periods was not explicitly considered.

This methodology has been applied to estimate the site-specific response spectrum at the location of the CTV building from the 22 February 2011 earthquake [36], where catastrophic structural collapse was observed claiming 185 lives [37]. Figure 6 illustrates the four closest strong motion stations which are part of the permanent GeoNet (www.geonet.org.nz) instrumentation network. These sites provide the principal 'constraints' in determining the conditional response spectrum at the CTV site because of their small separation distances, which are approximately 720m (CCCC), 1300m (REHS), 1250m (CHHC), and 1850m (CBGS).

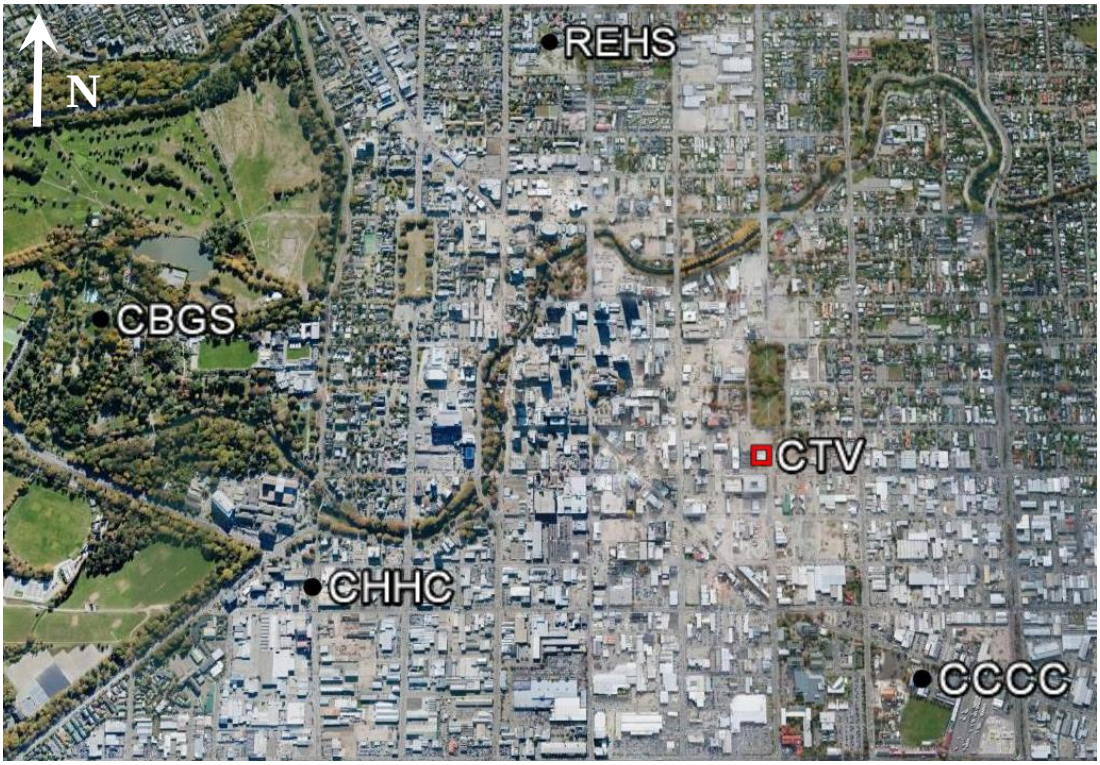

Accepted for publication, cite as: Bradley BA. Site-specific and spatially-distributed ground-motion intensity estimation in the 2010–2011 Canterbury earthquakes. *Soil Dynamics and Earthquake Engineering* 2014; **61–62** (0): 83-91.

Figure 6: Location of the four nearest strong motion stations to the CTV site that are part of the permanent GeoNet instrumentation program. CCCC = Christchurch Cathedral College; REHS =Christchurch Resthaven; CHHC = Christchurch Hospital; and CBGS = Christchurch Botanical Gardens. Image from Google Earth (last accessed: June 2013).

Figure 7 provides a comparison between the unconditional and conditional distributions of the ground motion response spectrum at the CTV site from the 22 February 2011 Christchurch earthquake. The unconditional response spectrum distribution is simply that predicted by the Bradley (2010) GMPE based on the location of the causative fault, the event magnitude, and the CTV site classification (site class D according to NZS1170.5:2004 [37, 38]), i.e. Equation (2). It can be seen that the median of the conditional response spectrum is generally greater than the median of the unconditional response spectrum (the exception being for $T < 0.3s$), as a result of the fact that the ground motions in the vicinity of the CTV site (e.g. CCCC, REHS, CHHC, CBGS), on average, had moderate-to-long period SA amplitudes slightly larger than that predicted by the Bradley (2010) GMPE [31]. Close comparison of the unconditional and conditional distributions also illustrates that there is a reduced standard deviation (i.e. depicted as a reduced difference between 16^{th}, 50^{th} (median), and 84^{th} percentiles) in the conditional distribution because of the additional information that has been utilized from the observed ground motions. This reduction in standard deviation is greatest at long vibration periods, since as previously noted, long period seismic waves have greater wavelengths and are therefore more coherent over a wider spatial region due to similar source, path and site effects.

Accepted for publication, cite as: Bradley BA. Site-specific and spatially-distributed ground-motion intensity estimation in the 2010–2011 Canterbury earthquakes. *Soil Dynamics and Earthquake Engineering* 2014; **61–62** (0): 83-91.

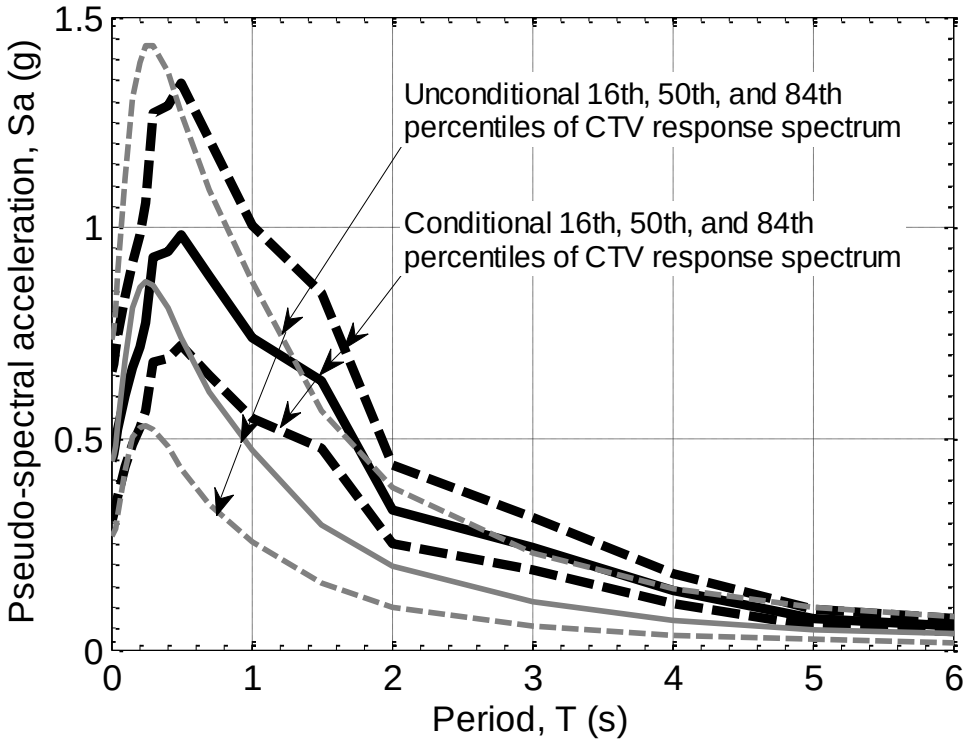

Figure 7: Comparison of unconditional and conditional geometric mean response spectra predicted at the CTV site from the 22 February 2011 Christchurch earthquake.

Figure 8 illustrates the median, 16th and 84th percentiles of the conditional response spectrum predicted at the site as well as the geometric mean response spectra of the four ground motions recorded in the general vicinity of the CTV site noted in Figure 6. It can be seen that, for the purposes of this particular application, the observed ground motions can be seen to provide a good representation of the conditional response spectrum at the CTV site, and therefore these ground motions were utilized in forensic response history analyses of the CTV structure, in lieu of direct ground motion records at that site [37].

Since cumulative effects from ground shaking prior to the 22 February 2011 Christchurch could have been a contributor to the collapse of the CTV building, ground motion time series from the 4 September 2010 earthquake were also desired for the purpose of performing sequential nonlinear seismic response analysis for both the 4 September 2010 and 22 February 2011 earthquakes. Figure 9 provides a comparison between the conditional response spectrum distribution predicted for the CTV site for the 4 September 2010 Darfield earthquake as well as the individual response spectra of the ground motions at the four stations in the vicinity of the CTV site. It can again be seen that these ground motions are also consistent with the conditional response spectra, and were therefore also considered appropriate for use in

forensic response history analyses of the CTV structure, in lieu of direct ground motion records at that site [37].

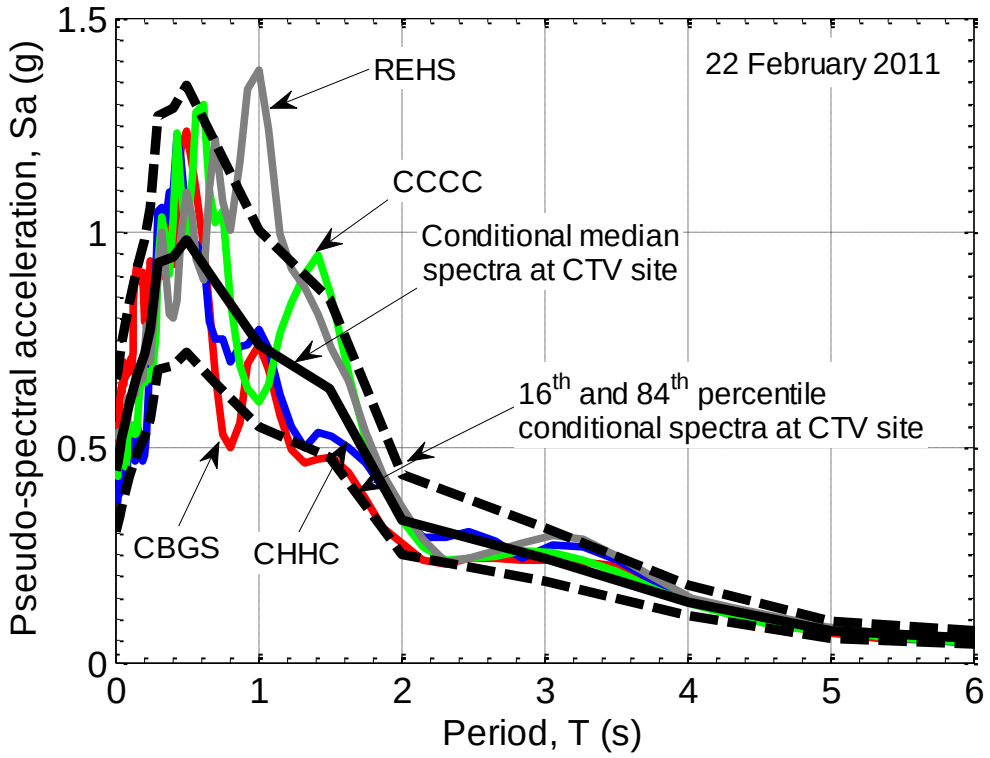

Figure 8: Comparison of the geometric mean response spectra of ground motions observed at the four 'CBD' strong motion stations (i.e. CCCC, CHHC, REHS, CBGS) with the conditional response spectrum distribution at the CTV site for the 22 February 2011 Christchurch earthquake (after Bradley [36]).

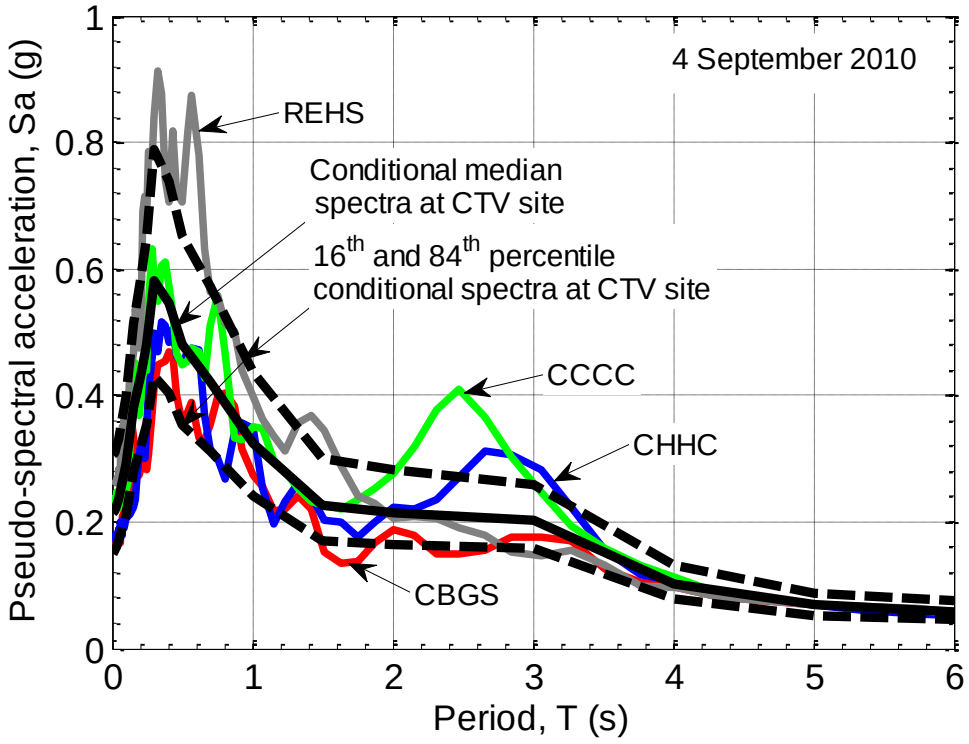

Figure 9: Comparison of the geometric mean response spectra of ground motions observed at the four 'CBD' strong motion stations (i.e. CCCC, CHHC, REHS, CBGS) with the conditional response spectrum distribution at the CTV site for the 4 September 2010 Darfield earthquake

Accepted for publication, cite as: Bradley BA. Site-specific and spatially-distributed ground-motion intensity estimation in the 2010–2011 Canterbury earthquakes. *Soil Dynamics and Earthquake Engineering* 2014; **61–62** (0): 83-91.
(after Bradley [36]).

CONCLUSIONS

This paper presents site-specific and spatially distributed ground motion intensity estimates which have been utilized in the aftermath of the 2010-2011 Canterbury, New Zealand earthquakes. The conditional distribution of ground motion intensity at a specific location is obtained on the basis of the (unconditional) prediction from empirical ground motion prediction equations; the observations of ground motion intensity at nearby strong motion stations; and the within-event spatial correlation of ground motion intensity. Empirical ground motion data from the Canterbury earthquakes were utilized to validate the adopted GMPE and within-event spatial correlation equations.

For the major seven earthquake events in the Canterbury earthquake sequence, maps of the median and standard deviation of the conditional distribution of peak ground acceleration were developed. The results embodied in such maps have been utilized for examining the liquefaction triggering potential of surficial soils in residential housing areas as part of land damage insurance assessments.

The conditional distribution of response spectral ordinates was also obtained at the location of the Canterbury Television building (CTV), which catastrophically collapsed in the 22 February 2011 earthquake. Among other things, the estimated conditional response spectra provide insight for the selection of ground motion records for use in forensic seismic response analyses of important structures at locations where direct recordings are absent.

ACKNOWLEDGMENTS

Christophe Loth and Jack Baker (Stanford University) kindly provided code which was used to compute the empirical semi-variograms utilized in the results given in Figure 3. Matthew Hughes (University of Canterbury) assisted in GIS-related aspects of the spatial PGA application. Financial support of the Ministry of Business, Innovation and Employment (MBIE), New Zealand Earthquake Commission (EQC) and New Zealand Natural Hazards Research Platform (NHRP) related to the spatial PGA application presented here is greatly appreciated. Any opinions, findings, and conclusions or recommendations expressed in this material are those of the author and do not necessarily reflect the views of the MBIE, EQC or NHRP. Constructive

comments from two anonymous reviewers are greatly appreciated.

REFERENCES

[1] Boore DM, Gibbs JF, Joyner WB, Tinsley JC and Ponti DJ. Estimated Ground Motion From the 1994 Northridge, California, Earthquake at the Site of the Interstate 10 and La Cienega Boulevard Bridge Collapse, West Los Angeles, California. *Bulletin of the Seismological Society of America* 2003; **93**(6): 2737-2751.

[2] Wang M and Takada T. Macrospatial Correlation Model of Seismic Ground Motions. *Earthquake Spectra* 2005; **21**(4): 1137-1156.

[3] Goda K and Hong HP. Spatial correlation of peak ground motions and response spectra. *Bulletin of the Seismological Society of America* 2008; **98**(1): 354-465.

[4] Jayaram N and Baker JW. Correlation model for spatially distributed ground-motion intensities. *Earthquake Engineering and Structural Dynamics* 2009; (in press). Published online 28 April 2009. DOI: 10.1002/eqe.922.

[5] Loth C and Baker JW. A spatial cross-correlation model of spectral accelerations at multiple periods. *Earthquake Engineering & Structural Dynamics* 2013; **42**(3): 397-417.

[6] Park J, Bazzurro P and Baker JW. *Modelling spatial correlation of ground motion intensity measures for regional seismic hazard and portfolio loss estimation*, in *9th International Conference on Application of Statistics and Probability in Civil Engineering*: Toyko, Japan, 2007, 8pp.

[7] Jayaram N. *Probabilistic seismic lifeline risk assessment using efficient sampling and data reduction techniques*, Ph.D in *Civil and Environmental Engineering*. Stanford University: Palo Alto, 2010, 311pp.

[8] Bommer JJ and Stafford PJ. Estimating ground motion levels in earthquake damage investigations: a framework for forensic engineering seismology. *International Journal of Forensic Engineering* 2012; **1**(1): 3-20.

[9] Stafford PJ. Evaluation of structural performance in the immediate aftermath of an earthquake: a case study of the 2011 Christchurch earthquake. *International Journal of Forensic Engineering* 2012; **1**(1): 58-77.

[10] Bhattacharya S and Goda K. Probabilistic buckling analysis of axially loaded piles in liquefiable soils. *Soil Dynamics and Earthquake Engineering* 2013; **45**(0): 13-24.

[11] Vanmarcke E. *Random Fields, Analysis and Synthesis*. The MIT Press: Cambridge, Massachussetts.

[12] Johnson RA and Wichern DW. *Applied Multivariate Statistical Analysis*. Prentice Hall: Upper Saddle River, NJ.

[13] Cubrinovski M, Bradley BA, Wotherspoon L, Green AG, Bray J, Wood C, Pender M, Allen CR, Bradshaw A, Rix G, Taylor M, Robinson K, Henderson D, Giorgini S, Ma K, Winkley A, Zupan J, O'Rourke TD, DePascale G and Wells DL. Geotechnical Aspects of the 22 February 2011 Christchurch Earthquake. *Bulletin of the New Zealand Society for Earthquake Engineering* 2011; **44**(4): 205-226.

[14] Cubrinovski M, Green RA, Allen J, Ashford SA, Bowman E, Bradley BA, Cox B, Hutchinson TC, Kavazanjian E, Orense RP, Pender M, Quigley M and Wotherspoon L. Geotechnical reconnaissance of the 2010 Darfield (Canterbury) earthquake. *Bulletin of the New Zealand Society for Earthquake*

Engineering 2010; **43**(4): 243-320.

[15] Quigley MC, Bastin S and Bradley BA. Recurrent liquefaction in Christchurch, New Zealand, during the Canterbury earthquake sequence. *Geology* 2013; **41**(4): 419-422.

[16] Cubrinovski M, Bray JD, Taylor M, Giorgini S, Bradley B, Wotherspoon L and Zupan J. Soil Liquefaction Effects in the Central Business District during the February 2011 Christchurch Earthquake. *Seismological Research Letters* 2011; **82**(6): 893-904.

[17] Canterbury Geotechnical Database. *https://canterburyrecovery.projectorbit.com/SitePages/Home.aspx*, 2011, pp.

[18] Idriss IM and Boulanger RW. *Soil Liquefaction During Earthquakes*. Earthquake Engineering Research Institute.

[19] Cubrinovski M, Hughes M, Bradley BA, MacCahon I, McDonald Y, Simpson H, Cameron R, Christison M, Henderson B, Orense R and O'Rouke TD. *Liquefaction impacts on pipe networks*, 2011. 78pp.

[20] Beavan J, Motagh M, Fielding EJ, Donnelly N and Collett D. Fault slip models of the 2010–2011 Canterbury, New Zealand, earthquakes from geodetic data and observations of postseismic ground deformation. *New Zealand Journal of Geology and Geophysics* 2012; **55**(3): 207-221.

[21] Ristau J. Implementation of routine regional moment tensor analysis in New Zealand. *Seismological Research Letters* 2008; **79**(3): 400-415.

[22] Stirling MW, Gerstenberger M, Litchfield N, McVerry GH, Smith WD, Pettinga JR and Barnes P. *Updated probabilistic seismic hazard assessment for the Canterbury region*, 2007. 58pp.

[23] Segou M and Kalkan E. Ground Motion Attenuation during M 7.1 Darfield and M 6.2 Christchurch, New Zealand, Earthquakes and Performance of Global Predictive Models. *Seismological Research Letters* 2011; **82**(6): 866-874.

[24] Bradley BA. Strong ground motion characteristics observed in the 4 September 2010 Darfield, New Zealand earthquake. *Soil Dynamics and Earthquake Engineering* 2012; **42**32-46.

[25] Bradley BA and Cubrinovski M. Near-source Strong Ground Motions Observed in the 22 February 2011 Christchurch Earthquake. *Seismological Research Letters* 2011; **82**(6): 853-865.

[26] Bradley BA. A New Zealand-Specific Pseudospectral Acceleration Ground-Motion Prediction Equation for Active Shallow Crustal Earthquakes Based on Foreign Models. *Bulletin of the Seismological Society of America* 2013; **103**(3): 1801-1822.

[27] Bradley BA. Systematic ground motion observations in the Canterbury earthquakes and region-specific non-ergodic empirical ground motion modeling. *Earthquake Spectra* 2013; **(submitted May 2013)**.

[28] Bradley BA. *NZ-specific pseudo-spectral acceleration ground motion prediction equations based on foreign models*, Report No.2010-03, Department of Civil and Natural Resources Engineering, University of Canterbury: Christchurch, New Zealand, 2010. 324pp.

[29] Bradley BA. A New Zealand-specific pseudo-spectral acceleration ground-motion prediction equation for active shallow crustal earthquakes based on foreign models. *Bulletin of the Seismological Society of America* 2013; **103**(3).

[30] Bradley BA. A critical analysis of strong ground motions observed in the 4 September 2010 Darfield earthquake. *Soil Dynamics and Earthquake*

Engineering 2012; ((accepted)).

[31] Bradley BA. *Systematic ground motion observations in the Canterbury earthquakes and region-specific non-ergodic empirical ground motion modelling*, Report No:2013-03, Department of Civil and Natural Resources Engineering, University of Canterbury: Christchurch, New Zealand, 2013. 74pp.

[32] Kawakami H and Mogi H. Analyzing Spatial Intraevent Variability of Peak Ground Accelerations as a Function of Separation Distance. *Bulletin of the Seismological Society of America* 2003; **93**(3): 1079-1090.

[33] Goda K and Atkinson GM. Intraevent Spatial Correlation of Ground-Motion Parameters Using SK-net Data. *Bulletin of the Seismological Society of America* 2010; **100**(6): 3055-3067.

[34] NZS 1170.5. *Structural design actions, Part 5: Earthquake actions - New Zealand*. Standards New Zealand: Wellington, New Zealand, 2004, 82pp.

[35] MBIE. *Guidelines for the investigation and assessment of subdivisions on the flat in Canterbury*, Ministry of Business, Innovation and Employment, 2012. 15pp.

[36] Bradley BA. *Ground motion aspects of the 22 February 2011 Christchurch earthquake related to the Canterbury Television (CTV) building*, 2012. 26pp.

[37] Canterbury Earthquakes Royal Commission. *Final Report: Volume 6: Canterbury Television Building (CTV)*, 2012. 324pp.

[38] Sinclair T. *CTV Building Geotechnical Advice*, 2012. 24pp.